JOURNAL OF NEUROTRAUMA 33:2133–2146 (December 1, 2016)

DOI: 10.1089/neu.2015.4267

Abnormalities in Diffusional Kurtosis Metrics Related to Head Impact Exposure in a Season of High School Varsity Football

Elizabeth M. Davenport,[1,2] Kalyna Apkarian,[4] Christopher T. Whitlow,[3,4,7] Jillian E. Urban,[4,8] Jens H. Jensen,[12] Eliza Szuch,[9] Mark A. Espeland,[5] Youngkyoo Jung,[3,4,8] Daryl A. Rosenbaum,[4] Gerard A. Gioia,[11] Alexander K. Powers,[6,10] Joel D. Stitzel,[4,7,8] and Joseph A. Maldjian[1,2]

Abstract

The purpose of this study was to determine whether the effects of cumulative head impacts during a season of high school football produce changes in diffusional kurtosis imaging (DKI) metrics in the absence of clinically diagnosed concussion. Subjects were recruited from a high school football team and were outfitted with the Head Impact Telemetry System (HITS) during all practices and games. Biomechanical head impact exposure metrics were calculated, including: total impacts, summed acceleration, and Risk Weighted Cumulative Exposure (RWE). Twenty-four players completed pre- and post-season magnetic resonance imaging, including DKI; players who experienced clinical concussion were excluded. Fourteen subjects completed pre- and post-season Immediate Post-Concussion Assessment and Cognitive Testing (ImPACT). DKI-derived metrics included mean kurtosis (MK), axial kurtosis (K axial), and radial kurtosis (K radial), and white matter modeling (WMM) parameters included axonal water fraction, tortuosity of the extra-axonal space, extra-axonal diffusivity (D_e axial and radial), and intra-axonal diffusivity (D_a). These metrics were used to determine the total number of abnormal voxels, defined as 2 standard deviations above or below the group mean. Linear regression analysis revealed a statistically significant relationship between RWE combined probability (RWE_{CP}) and MK. Secondary analysis of other DKI-derived and WMM metrics demonstrated statistically significant linear relationships with RWE_{CP} after covariate adjustment. These results were compared with the results of DTI-derived metrics from the same imaging sessions in this exact same cohort. Several of the DKI-derived scalars (D_a, MK, K axial, and K radial) explained more variance, compared with RWE_{CP}, suggesting that DKI may be more sensitive to subconcussive head impacts. No significant relationships between DKI-derived metrics and ImPACT measures were found. It is important to note that the pathological implications of these metrics are not well understood. In summary, we demonstrate a single season of high school football can produce DKI measurable changes in the absence of clinically diagnosed concussion.

Keywords: concussion; diffusion kurtosis imaging; football; Head Impact Telemetry System; Risk Weighted Cumulative Exposure

Introduction

Football has the highest concussion rate of any competitive contact sport.[1] Parents, coaches, and physicians of youth athletes are becoming increasingly concerned about the effects of head impacts. These concerns are reflected in the recent 9.5% decrease in participation in the Pop Warner youth football program.[2] While concussion can represent a serious and immediate clinical manifestation of any head impact, the effects of repeated subconcussive impacts on youth and high school populations are largely unknown.

Previous research has focused primarily on collegiate football players.[3–7] Recent biomechanical studies of head impacts have shown impact distributions for youth and high school players to be

[1]Advanced Neuroscience Imaging Research (ANSIR) Laboratory, [2]Department of Radiology, [3]Department of Radiology-Neuroradiology, [4]Department of Biomedical Engineering, [5]Department of Biostatistical Sciences, [6]Department of Neurosurgery, [7]Translational Science Institute, [8]Virginia Tech-Wake Forest School of Biomedical Engineering, [9]MD Program, [10]Childress Institute for Pediatric Trauma, Wake Forest School of Medicine, Winston-Salem, North Carolina.
[11]Division of Pediatric Neuropsychology, Children's National Medical Center, George Washington University School of Medicine, Rockville, Maryland.
[12]Department of Radiology and Radiological Science, Center for Biomedical Imaging, Medical University of South Carolina, Charleston, South Carolina.

similar to those seen at the collegiate level, with differences primarily in the highest impact magnitudes and total number of impacts.[7–9] The effects of these impacts can, in part, be studied through measuring the integrity of white matter, or using diffusion tensor imaging (DTI) derived metrics, which are known to be important in tracking brain development.[10] Recently, we demonstrated associations between DTI-derived metric changes and biomechanical head impact metrics over a single season of high school football.[11] Bazarian and colleagues found similar changes in DTI-derived metrics that correlated with helmet impact measures over a single season of collegiate football.[12]

Diffusional kurtosis imaging (DKI) is an extension of DTI that may provide additional information regarding white matter integrity. When diffusion is homogeneous and Gaussian, it can be calculated using the linear estimation methods applied for DTI. However, diffusion in the brain is naturally anisotropic and non-Gaussian due to the effects of the cellular microstructure, particularly myelinated axons. DKI is able to measure the non-Gaussian diffusion by requiring three b values and at least 15 gradient directions. Kurtosis refers, in general, to a dimensionless statistic that quantifies the deviation from a Gaussian, or normal distribution.[13] Kurtosis can be used to characterize quantitatively non-Gaussian water diffusion from magnetic resonance imaging (MRI) using a series of equations.[14] The diffusional kurtosis pertains specifically to the distribution of molecular displacements associated with a diffusive medium, such as water within brain tissue. A greater degree of structure in the medium tends to cause more deviations from Gaussian movement and typically increases the diffusional kurtosis.[15] Because water diffusion in the brain is anisotropic, particularly in white matter, the diffusional kurtosis depends on the direction in which the diffusion is measured.

DKI-derived metrics include mean kurtosis (MK), axial kurtosis (K axial), and radial kurtosis (K radial).[16] MK is the mean, over all diffusion directions, of the measured diffusional kurtosis. K axial is measured along the principal diffusion tensor eigenvector, while K radial is the average measured kurtosis over all directions perpendicular to the principal eigenvector. The principal diffusion tensor eigenvector is the direction that maximizes the diffusivity; in white matter regions with unidirectional axons, it generally will be oriented parallel to the axons, which is the basis of white matter fiber tractography.[17]

These kurtosis parameters apply to any diffusive medium and reflect the physics of the diffusion dynamics. By augmenting these with tissue modeling assumptions for brain microstructure, additional metrics can be calculated that have more specific biological interpretations.[18] One simple example, which we call the white matter modeling (WMM) method, assumes that the axons are unidirectional and that brain tissue water can effectively be divided into two non-exchanging pools corresponding to the intra-axonal space and extra-axonal space (EAS).[31] The combination of DKI and WMM allows for the calculation of several model parameters, including the axonal water fraction (AWF), the tortuosity of the EAS, the extra-axonal diffusivities (D_e axial and radial), and the intra-axonal diffusivity. AWF represents the fraction of the water signal in the axons relative to the total water signal. Tortuosity measures the ratio of diffusion along the direction of the fibers and the diffusion perpendicular to the fibers in the EAS; it is expected to be sensitive to the myelinated axonal fraction, which increases with increasing myelin and axonal density.

DKI-derived metrics have been used to study early development, autism spectrum disorders, attention-deficit/hyperactivity disorder, Alzheimer's disease, and traumatic brain injury (TBI).[19–23] These studies suggest that DKI-derived metrics can provide a more sensitive imaging biomarker to assess the changes in microstructure in the brain. MK increases with age, as expected for brain development; however, other metrics are not well studied in the adolescent age group.[19,22] Stokum and colleagues showed decreases in MK and K radial, from 10 days post-injury to 6 months post-injury, in subjects with TBI, compared with controls.[21] Grossman and colleagues also showed decreases in MK in subjects scanned within 1 year post-injury, compared with controls.[24] In contrast, Zhuo and colleagues showed increases in MK from baseline in rats scanned 7 days post-injury, which coincided with increases in K axial and decreases in K radial.[25]

Concussion, or mild traumatic brain injury (mTBI), is typically a clinical diagnosis. However, in order to study the more subtle effects of subconcussive head impacts, an effective method of measuring the biomechanical forces associated with each head impact is required. To acquire this information, many investigators have used the Head Impact Telemetry System (HITS). The HITS collects real-time data during on-field play, and has been implemented at the youth, high school, and collegiate levels.[3–6,8,26,27] It consists of a base unit, placed beside the field, and helmet-embedded encoders that are designed such that the sensors remain in contact with the head to ensure measurement of head acceleration rather than helmet acceleration. These helmet-embedded sensor systems collect data on number of impacts, time between impacts, as well as peak resultant linear acceleration and estimated peak resultant rotational acceleration, which is sent to the base unit in real-time. This data is then analyzed in terms of the peak acceleration, impact location, and other biomechanical indicators.

The primary aim of this study was to determine if the cumulative effects of head impacts from a season of high school varsity football can produce DKI detectable changes in the brain in the absence of clinically diagnosed concussion. The primary hypothesis was that there would be a significant association between the cumulative head impact exposure of an athlete and DKI-derived metrics, due to an alteration in microstructural complexity related to axonal injury.[25] Additionally, we compared the DKI metrics to DTI metrics from a previous study computed in the same cohort.

Methods

Protocol summary

The HITS data collection, imaging acquisition, cognitive testing, and subjects for this paper are identical to that of Davenport and colleagues[11] and are abbreviated here.[7] The calculation of DKI scalar metrics differs and is explained in more detail.

All subjects ($n = 24$, male; mean age = 16.9) were fitted with the HITS for acquisition of biomechanical exposure data during all practices and games. From this data, Risk Weighted Cumulative Exposure (RWE) was calculated.[7] This metric represents the cumulative concussion risk for each impact for each player over the course of the season. The RWE can be calculated separately from the linear, rotational, and combined probability risk functions and is referred to as RWE_{Linear}, $RWE_{Rotational}$, and RWE_{CP} respectively.[28,29] Our primary hypothesis relates to changes in the brain associated with RWE_{CP}. RWE_{CP} is based on the combined probability associated with the peak resultant linear and rotational acceleration components of each head impact. In addition, all participants received baseline, pre-season, and post-season MRI and ImPACT neuropsychologic testing.

Table 1A. Associations Between HITS Metrics and Changes in WMM Metrics in White Matter Areas with FA >0.4 (± SD 2.0)

	Without covariate adjustment		*Covariate adjustment for age, BMI, and time between scans*		
	R^2	*p value*	*Adjusted* R^2	*Covariate-adjusted* R^2	*p value*
AWF vs. RWE_{CP}	0.2039	**0.0268***	0.5069	0.5237	**0.0013***
Tortuosity vs. RWE_{CP}	0.1895	**0.0335***	0.3401	0.4050	**0.0167***
D_e axial vs. RWE_{CP}	0.1799	**0.0389***	0.4212	0.4513	**0.0054***
D_e radial vs. RWE_{CP}	0.1410	0.0706	0.4209	0.4193	**0.0054***
D_a vs. RWE_{CP}	0.2391	**0.0153***	0.6412	0.6415	**< 0.0001***
AWF vs. RWE_{Linear}	0.0839	0.1697	0.2861	0.3105	**0.0324***
Tort vs. RWE_{Linear}	0.0666	0.2233	0.1354	0.2204	0.1518
D_e axial vs. RWE_{Linear}	0.0614	0.2432	0.2198	0.2603	0.0675
D_e radial vs. RWE_{Linear}	0.0491	0.2979	0.3085	0.3066	**0.0248***
D_a vs. RWE_{Linear}	0.0830	0.1721	0.3944	0.3949	**0.0080***
AWF vs. $RWE_{Rotational}$	0.0840	0.1696	0.0946	0.1255	0.2151
Tortuosity vs. $RWE_{Rotational}$	0.0683	0.2173	0.0101	0.1074	0.4039
D_e axial vs. $RWE_{Rotational}$	0.0880	0.1593	0.1038	0.1504	0.1993
D_e radial vs. $RWE_{Rotational}$	0.0871	0.1615	0.2358	0.2336	0.0570
D_a vs. $RWE_{Rotational}$	0.0064	0.7096	0.0295	0.0304	0.3532
AWF vs. total impacts	0.0127	0.5997	0.0034	0.0374	0.4225
Tortuosity vs. total impacts	0.0110	0.6264	–0.0654	0.0393	0.6358
D_e axial vs. total impacts	0.0041	0.7664	–0.0222	0.0310	0.4970
D_e radial vs. total impacts	0.0018	0.8448	0.0701	0.0675	0.2614
D_a vs. total impacts	0.0067	0.7033	0.0672	0.0680	0.2674
AWF vs. summed linear acceleration	0.0244	0.4664	0.0504	0.1181	0.3037
Tortuosity vs. summed linear acceleration	0.0182	0.5296	–0.0340	0.1054	0.5335
D_e axial vs. summed linear acceleration	0.0116	0.6171	0.0175	0.1138	0.3841
D_e radial vs. summed linear acceleration	0.0078	0.6812	0.1224	0.2173	0.1701
D_a vs. summed linear acceleration	0.0167	0.5476	0.1281	0.2151	0.1619
AWF vs. summed rotational acceleration	0.0232	0.4774	0.0434	0.1072	0.3196
Tortuosity vs. summed rotational acceleration	0.0203	0.5067	–0.0337	0.1029	0.5327
D_e axial vs. summed rotational acceleration	0.0104	0.6349	0.0081	0.0982	0.4092
D_e radial vs. summed rotational acceleration	0.0072	0.6929	0.1072	0.1902	0.1936
D_a vs. summed rotational acceleration	0.0203	0.5062	0.1318	0.2152	0.1567

*$p < 0.05$. Bold p values.

HITS, Head Impact Telemetry System; WMM, white matter modeling; FA, fractional anisotropy; SD, standard deviation; BMI, body mass index; AWF, axonal water fraction; RWEcp, Risk Weighted Cumulative Exposure combined probability; D_e axial and radial, extra-axonal diffusivity; D_a, intra-axonal diffusivity.

Table 1B. Associations Between HITS Metrics and Changes in DKI-Derived Metrics in WHOLE BRAIN (± SD 2.0)

	Without covariate adjustment		*Covariate adjustment for age, BMI, and time between scans*		
	R^2	*p value*	*Adjusted* R^2	*Covariate-adjusted* R^2	*p value*
MK vs. RWE_{CP}	0.0397	0.3507	0.6598	0.4572	**< 0.0001***
K axial vs. RWE_{CP}	0.0578	0.2577	0.6284	0.4712	**0.0001***
K radial vs. RWE_{CP}	0.0302	0.4169	0.5933	0.3760	**0.0002***
MK vs. RWE_{Linear}	0.0038	0.7738	0.6079	0.3745	**0.0002***
K axial vs. RWE_{Linear}	0.0109	0.6267	0.5732	0.3926	**0.0004***
K radial vs. RWE_{Linear}	0.0015	0.8580	0.5508	0.3108	**0.0006***
MK vs. $RWE_{Rotational}$	0.0591	0.2523	0.5014	0.2045	**0.0014***
K axial vs. $RWE_{Rotational}$	0.0397	0.3503	0.4019	0.1487	**0.0072***
K radial vs. $RWE_{Rotational}$	0.0552	0.2691	0.4811	0.2039	**0.0021***
MK vs. total impacts	0.0066	0.7055	0.5297	0.2497	**0.0009***
K axial vs. total impacts	0.0116	0.6166	0.4770	0.2557	**0.0022***
K radial vs. total impacts	0.0051	0.7402	0.5023	0.2364	**0.0014***
MK vs. summed linear acceleration	0.0051	0.7405	0.5466	0.4444	**0.0006***
K axial vs. summed linear acceleration	0.0099	0.6430	0.4977	0.4482	**0.0015***
K radial vs. summed linear acceleration	0.0031	0.7949	0.5112	0.413935	**0.0012***
MK vs. summed rotational acceleration	0.0103	0.6373	0.5548	0.4456	**0.0005***
K axial vs. summed rotational acceleration	0.0165	0.5502	0.5063	0.4517	**0.0013***
K radial vs. summed rotational acceleration	0.0071	0.6961	0.5169	0.4141	**0.0011***

*$p < 0.05$. Bold p values.

HITS, Head Impact Telemetry System; DKI, diffusional kurtosis imaging; SD, standard deviation; BMI, body mass index; MK, mean kurtosis; RWEcp, Risk Weighted Cumulative Exposure combined probability; K axial, axial kurtosis; K radial, radial kurtosis.

Table 1C. Associations Between HITS Metrics and Changes in DKI-Derived Metrics in White Matter (± SD 2.0)

	Without covariate adjustment		*Covariate adjustment for age, BMI, and time between scans*		
	R^2	*p value*	*Adjusted* R^2	*Covariate-adjusted* R^2	*p value*
MK vs. RWE_{CP}	0.1411	0.0705	0.4993	0.4807	**0.0015***
K axial vs. RWE_{CP}	0.1891	**0.0337***	0.5735	0.5597	**0.0004***
K radial vs. RWE_{CP}	0.1474	0.0640	0.4024	0.4194	**0.0071***
MK vs. RWE_{Linear}	0.0347	0.3837	0.2699	0.2427	**0.0391***
K axial vs. RWE_{Linear}	0.0398	0.3497	0.3342	0.3126	**0.0180***
K radial vs. RWE_{Linear}	0.0443	0.3233	0.3438	0.2283	0.0779
MK vs. $RWE_{Rotational}$	0.0769	0.1894	0.1604	0.1291	0.1210
K axial vs. $RWE_{Rotational}$	0.0004	0.9252	0.0642	0.0339	0.2736
K radial vs. $RWE_{Rotational}$	0.0612	0.2438	0.0713	0.0977	0.2590
MK vs. total impacts	0.0073	0.6923	0.0739	0.0394	0.2539
K axial vs. total impacts	0.0006	0.9134	0.0714	0.0413	0.2588
K radial vs. total impacts	0.0128	0.5984	0.0253	0.0530	0.3640
MK vs. summed linear acceleration	0.0104	0.6360	0.1036	0.1116	0.1996
K axial vs. summed linear acceleration	0.0001	0.0029	0.1084	0.1670	0.1917
K radial vs. summed linear acceleration	0.0170	0.3798	0.0554	0.1288	0.2926
MK vs. summed rotational acceleration	0.0129	0.5972	0.1072	0.1143	0.1937
K axial vs. summed rotational acceleration	0.0005	0.9178	0.1085	0.1630	0.1916
K radial vs. summed rotational acceleration	0.0197	0.5129	0.0572	0.1279	0.2886

*$p < 0.05$. Bold p values.

HITS, Head Impact Telemetry System; DKI, diffusional kurtosis imaging; SD, standard deviation; BMI, body mass index; MK, mean kurtosis; RWEcp, Risk Weighted Cumulative Exposure combined probability; K axial, axial kurtosis; K radial, radial kurtosis.

ImPACT cognitive testing protocol

Neuropsychological testing was administered pre- and post-season using version 2.1 of the ImPACT computer test battery at the high school computer laboratory under the supervision of the team's athletic trainer.[30,31] Ten of the 24 subjects did not return for post-season ImPACT testing, leaving 14 subjects (mean age, 17.03) with complete pre- and post-season testing. The outcome measures include Verbal Memory, Visual Memory, Visual Motor (Processing Speed), and Reaction Time.

MRI acquisition and processing

MRI data was acquired on a 3 Tesla Siemens Skyra MRI scanner using a 32-channel human head/neck coil (Siemens Medical,

Table 1D. Associations Between HITS Metrics and Changes in DKI-Derived Metrics in Gray Matter (± SD 2.0)

	Without covariate adjustment		*Covariate adjustment for age, BMI, and time between scans*		
	R^2	*p value*	*Adjusted* R^2	*Covariate-Adjusted* R^2	*p value*
MK vs. RWE_{CP}	0.0271	0.4419	0.6575	0.4182	**< 0.0001***
K axial vs. RWE_{CP}	0.0455	0.3171	0.6125	0.4339	**0.0001***
K radial vs. RWE_{CP}	0.0199	0.5112	0.5975	0.3443	**0.0002***
MK vs. RWE_{Linear}	0.0018	0.8449	0.6328	0.3762	**< 0.0001***
K axial vs. RWE_{Linear}	0.0081	0.6767	0.5747	0.3786	**0.0003***
K radial vs. RWE_{Linear}	0.0003	0.9360	0.5756	0.3086	**0.0003***
MK vs. $RWE_{Rotational}$	0.0539	0.2751	0.5336	0.2077	**0.0008***
K axial vs. $RWE_{Rotational}$	0.0431	0.3306	0.4218	0.1552	**0.0053***
K radial vs. $RWE_{Rotational}$	0.0517	0.2853	0.5168	0.2127	**0.0011***
MK vs. total impacts	0.0067	0.7033	0.5841	0.2934	**0.0003***
K axial vs. total impacts	0.0135	0.5890	0.5052	0.2771	**0.0013***
K radial vs. total impacts	0.0047	0.7508	0.5515	0.2693	**0.0006***
MK vs. summed linear acceleration	0.0047	0.7505	0.5964	0.4562	**0.0002***
K axial vs. summed linear acceleration	0.0108	0.6293	0.5210	0.4645	**0.0010***
K radial vs. summed linear acceleration	0.0024	0.8186	0.5558	0.4500	**0.0005***
MK vs. summed rotational acceleration	0.0100	0.6437	0.6042	0.4918	**0.0002***
K axial vs. summed rotational acceleration	0.0178	0.5338	0.5305	0.4692	**0.0008***
K radial vs. summed rotational acceleration	0.0062	0.7157	0.5614	0.4499	**0.0005***

*$p < 0.05$. Bold p values.

HITS, Head Impact Telemetry System; DKI, diffusional kurtosis imaging; SD, standard deviation; BMI, body mass index; MK, mean kurtosis; RWEcp, Risk Weighted Cumulative Exposure combined probability; K axial, axial kurtosis; K radial, radial kurtosis.

Erlangen, Germany) in accordance with the National Institute of Neurological Disorders and Stroke Common Data Elements specification. T1-weighted images were obtained for anatomic correlation using a 3D volumetric Magnetization Prepared Rapid Acquisition Gradient Echo sequence with isotropic resolution of 0.9 mm^3: repetition time (TR) = 1900 msec; echo time (TE) = 2.93 msec; inversion time (TI) = 900 msec; flip angle = 9 degrees; slices = 176. Diffusion-weighted data were acquired using a two-dimensional single-shot EPI sequence (TR = 10,500 msec; TE = 99 msec; flip angle = 90 degrees; spatial resolution = $2.2 \times 2.2\ mm^2$; slice thickness = 3 mm; slices = 54; 10 b = 0 volumes; 15 diffusion directions with b = 1000/2000 sec/mm^2 each). The additional b value of 2000 provided for computation of DKI metrics.

Pre-processing of diffusion tensor images was performed using FMRIB Software Library.[32] All DKI-derived and WMM metrics were calculated using the Diffusion Kurtosis Estimator (DKE).[33] Images were corrected for distortion by normalizing the B0 image to the T1 image and subsequently applying the transform to the DKE output images. These scalar maps were then normalized to MNI space based on parameters from an SPM8 normalization of the corresponding T1-weighted structural images. WMM metrics were masked to only allow white matter voxels with fractional anisotropy (FA) above 0.4, in accordance with the model assumptions.[34] DKI-derived metrics were masked for whole–brain, white matter, and gray matter for separate analysis. All images were visually inspected to ensure quality of processing procedures. Delta maps (post-season minus pre-season), were computed for each DKI and WMM metric. The group mean and standard deviation of the delta maps were used to calculate voxel-wise Z-scores thresholded at ±2 SD.[11] This provides a single number representing the total number of abnormal voxels for each subject and each scalar metric to be used in the regression analysis.

Comparison of biomechanics and imaging data

Linear regression analyses were performed to study the relationship between cumulative exposure metrics and DKI-derived and WMM metrics using JMP (SAS Institute Inc., Cary, NC). Secondary analyses with RWE_{Linear} and $RWE_{Rotational}$, and DKI-derived and WMM measures also were performed to better characterize any associations. In the primary analysis, the number of abnormal MK voxels was used as a dependent variable. A log transformation was applied in order to satisfy assumptions of normality. Age at pre-season, body mass index (BMI), and time between scans were used as covariates. No outliers were identified in any linear regression performed based on the Cook's distance of each point.

Table 2A. Associations Between HITS Metrics and Changes in WMM Metrics in White Matter Areas With FA >0.4 (> 2 SD)

	Without covariate adjustment		*Covariate adjustment for age, BMI, and time between scans*		
	R^2	*p value*	*Adjusted* R^2	*Covariate-adjusted* R^2	*p value*
AWF vs. RWE_{CP}	0.2129	**0.0232***	0.3937	0.4438	**0.0081***
Tortuosity vs. RWE_{CP}	0.1107	0.1122	0.1578	0.2528	0.1239
D_e axial vs. RWE_{CP}	0.1549	0.0571	0.3412	0.3494	**0.0165***
D_e radial vs. RWE_{CP}	0.1285	0.0854	0.4076	0.3927	**0.0066***
D_a vs. RWE_{CP}	0.2485	**0.0132***	0.5408	0.5609	**0.0007***
AWF vs. RWE_{Linear}	0.0459	0.3146	0.1443	0.2150	0.1402
Tort vs. RWE_{Linear}	0.0337	0.3902	0.0321	0.1412	0.3469
D_e axial vs. RWE_{Linear}	0.0703	0.2106	0.2102	0.2200	0.0744
D_e radial vs. RWE_{Linear}	0.0554	0.2683	0.2858	0.2679	**0.0326***
D_a vs. RWE_{Linear}	0.0795	0.1819	0.3142	0.3442	**0.0232***
AWF vs. $RWE_{Rotational}$	0.0145	0.5756	0.1013	0.0019	0.7116
Tortuosity vs. $RWE_{Rotational}$	0.0255	0.4560	–0.0637	0.0562	0.6303
D_e axial vs. $RWE_{Rotational}$	0.0922	0.1492	0.0565	0.0682	0.2900
D_e radial vs. $RWE_{Rotational}$	0.1113	0.1112	0.1525	0.1312	0.1302
D_a vs. $RWE_{Rotational}$	0.0001	0.9635	0.1406	0.0052	0.5537
AWF vs. total impacts	0.0004	0.9298	–0.0635	0.0243	0.6295
Tortuosity vs. total impacts	0.0038	0.7749	–0.0951	0.0283	0.7357
D_e axial vs. total impacts	0.0159	0.5575	0.0282	0.0402	0.3566
D_e radial vs. total impacts	0.0071	0.6964	0.0594	0.0358	0.2838
D_a vs. total impacts	0.0027	0.8086	0.0256	0.0683	0.3632
AWF vs. summed linear acceleration	0.0003	0.9395	–0.0389	0.1024	0.5491
Tortuosity vs. summed linear acceleration	0.0067	0.7039	–0.0756	0.0815	0.6699
D_e axial vs. summed linear acceleration	0.0315	0.4069	0.0682	0.0928	0.2653
D_e radial vs. summed linear acceleration	0.0175	0.5381	0.1029	0.1166	0.2008
D_a vs. summed linear acceleration	0.0109	0.6278	0.0804	0.2155	0.2411
AWF vs. summed rotational acceleration	0.0017	0.8463	–0.0292	0.1137	0.5187
Tortuosity vs. summed rotational acceleration	0.0097	0.6463	–0.0693	0.0873	0.6488
D_e axial vs. summed rotational acceleration	0.0339	0.3891	0.0637	0.0823	0.2746
D_e radial vs. summed rotational acceleration	0.0152	0.5666	0.0884	0.0921	0.2261
D_a vs. summed rotational acceleration	0.0173	0.5397	0.0935	0.2263	0.2169

*$p < 0.05$ Bold p values.

HITS, Head Impact Telemetry System; WMM, white matter modeling; FA, fractional anisotropy; SD, standard deviation; BMI, body mass index; AWF, axonal water fraction; RWEcp, Risk Weighted Cumulative Exposure combined probability; D_e axial and radial, extra-axonal diffusivity; D_a, intra-axonal diffusivity.

Table 2B. Associations Between HITS Metrics and Changes in DKI-Derived Metrics in Whole–Brain (> 2 SD)

	Without covariate adjustment		*Covariate adjustment for age, BMI, and time between scans*		
	R^2	*p value*	*Adjusted* R^2	*Covariate-adjusted* R^2	*p value*
MK vs. RWE_{CP}	0.0942	0.1446	0.4630	0.3523	**0.0028***
K axial vs. RWE_{CP}	0.1163	0.1030	0.4830	0.4052	**0.0020***
K radial vs. RWE_{CP}	0.0738	0.1992	0.4675	0.3208	**0.0026***
MK vs. RWE_{Linear}	0.0285	0.4304	0.3073	0.1645	**0.0252***
K axial vs. RWE_{Linear}	0.0469	0.3092	0.3165	0.2136	**0.0225***
K radial vs. RWE_{Linear}	0.0216	0.4934	0.3391	0.1570	**0.0169***
MK vs. $RWE_{Rotational}$	0.0772	0.1888	0.1828	0.0143	0.0978
K axial vs. $RWE_{Rotational}$	0.1044	0.1236	0.1649	0.0391	0.1160
K radial vs. $RWE_{Rotational}$	0.0655	0.2273	0.2210	0.0063	0.0666
MK vs. total impacts	0.0265	0.4473	0.2058	0.0421	0.0778
K axial vs. total impacts	0.0463	0.3125	0.1876	0.0653	0.0933
K radial vs. total impacts	0.0253	0.4578	0.2534	0.0476	**0.0471***
MK vs. summed linear acceleration	0.0313	0.4084	0.2251	0.0294	0.0638
K axial vs. summed linear acceleration	0.0495	0.2963	0.2099	0.0652	0.0747
K radial vs. summed linear acceleration	0.0291	0.4254	0.2711	0.0295	**0.0386***
MK vs. summed rotational acceleration	0.0379	0.3623	0.2289	0.0304	0.0613
K axial vs. summed rotational acceleration	0.0572	0.2603	0.2154	0.0681	0.0706
K radial vs. summed rotational acceleration	0.0351	0.3804	0.2735	0.0281	**0.0376***

*$p < 0.05$. Bold p values.

HITS, Head Impact Telemetry System; DKI, diffusional kurtosis imaging; SD, standard deviation; BMI, body mass index; MK, mean kurtosis; RWEcp, Risk Weighted Cumulative Exposure combined probability; K axial, axial kurtosis; K radial, radial kurtosis.

No corrections were made for multiple comparisons, as our primary hypothesis centered on the relationship between RWE and MK.

Comparison of cognitive testing and imaging data

The delta (post- season minus pre-season) of each ImPACT outcome measure also was computed (Verbal Memory, Visual Memory, Visual Motor [Processing Speed], and Reaction Time). The delta scores were then individually, compared with the number of abnormal DKI voxels using the Spearman's rank correlation coefficient.

Results

Our primary hypothesis focused on changes in MK associated with RWE_{CP}. This association explained 4% of the total variance in

Table 2C. Associations Between HITS Metrics and Changes in DKI-Derived Metrics in White Matter (> 2 SD)

	Without covariate adjustment		*Covariate adjustment for age, BMI, and time between scans*		
	R^2	*p value*	*Adjusted* R^2	*Covariate-adjusted* R^2	*p value*
MK vs. RWE_{CP}	0.1010	0.1302	0.3240	0.3166	**0.0205***
K axial vs. RWE_{CP}	0.1818	**0.0378***	0.4917	0.4924	**0.0017***
K radial vs. RWE_{CP}	0.1119	0.1102	0.3032	0.3200	**0.0265***
MK vs. RWE_{Linear}	0.0001	0.9803	0.0793	0.0692	0.2433
K axial vs. RWE_{Linear}	0.0152	0.5660	0.1836	0.1847	0.0970
K radial vs. RWE_{Linear}	0.0032	0.7937	0.0777	0.1000	0.2463
MK vs. $RWE_{Rotational}$	0.0628	0.2376	0.0723	0.0622	0.2570
K axial vs. $RWE_{Rotational}$	0.0082	0.6742	–0.0012	0.0001	0.4354
K radial vs. $RWE_{Rotational}$	0.0558	0.2664	0.0351	0.0584	0.3395
MK vs. total impacts	0.0370	0.03679	0.0113	0.0005	0.4006
K axial vs. total impacts	0.0155	0.5621	0.0019	0.0032	0.4265
K radial vs. total impacts	0.0169	0.5450	–0.0239	0.0009	0.5022
MK vs. summed linear acceleration	0.0273	0.4407	0.0118	0.0004	0.3993
K axial vs. summed linear acceleration	0.0078	0.6812	0.1866	0.0588	0.3898
K radial vs. summed linear acceleration	0.0111	0.6227	0.1590	0.0223	0.4845
MK vs. summed rotational acceleration	0.0163	0.5527	0.0152	0.0157	0.3903
K axial vs. summed rotational acceleration	0.0039	0.7710	0.0208	0.0605	0.3754
K radial vs. summed rotational acceleration	0.0059	0.7204	–0.0136	0.0329	0.4712

* $p < .05$. Bold p values.

HITS, Head Impact Telemetry System; DKI, diffusional kurtosis imaging; SD, standard deviation; BMI, body mass index; MK, mean kurtosis; RWEcp, Risk Weighted Cumulative Exposure combined probability; K axial, axial kurtosis; K radial, radial kurtosis.

TABLE 2D. ASSOCIATIONS BETWEEN HITS METRICS AND CHANGES IN DKI-DERIVED METRICS IN GRAY MATTER (> 2 SD)

	Without covariate adjustment		*Covariate adjustment for age, BMI, and time between scans*		
	R^2	*p value*	*Adjusted* R^2	*Covariate-adjusted* R^2	*p value*
MK vs. RWE_{CP}	0.0849	0.1671	0.4412	0.3193	**0.0040***
K axial vs. RWE_{CP}	0.1077	0.1174	0.4590	0.3729	**0.0030***
K radial vs. RWE_{CP}	0.0608	0.2454	0.4372	0.2769	**0.0042***
MK vs. RWE_{Linear}	0.0333	0.3937	0.3106	0.1602	**0.0242***
K axial vs. RWE_{Linear}	0.0508	0.2898	0.3095	0.1996	**0.0245***
K radial vs. RWE_{Linear}	0.0216	0.4927	0.3324	0.1424	**0.0184***
MK vs. $RWE_{Rotational}$	0.0985	0.1352	0.1952	0.0196	0.0866
K axial vs. $RWE_{Rotational}$	0.1204	0.0966	0.1712	0.0393	0.1093
K radial vs. $RWE_{Rotational}$	0.0826	0.1734	0.2294	0.0101	0.0610
MK vs. total impacts	0.0397	0.3507	0.2195	0.0492	0.0676
K axial vs. total impacts	0.0594	0.2512	0.1938	0.0655	0.0878
K radial vs. total impacts	0.0332	0.3944	0.2604	0.0499	**0.0435***
MK vs. summed linear acceleration	0.0442	0.3239	0.2382	0.0181	0.0555
K axial vs. summed linear acceleration	0.0617	0.2420	0.2143	0.0421	0.0714
K radial vs. summed linear acceleration	0.0363	0.3724	0.2766	0.0148	**0.0362***
MK vs. summed rotational acceleration	0.0507	0.2899	0.2409	0.0174	0.0539
K axial vs. summed rotational acceleration	0.0693	0.2141	0.2193	0.0447	0.0678
K radial vs. summed rotational acceleration	0.0419	0.3374	0.2778	0.0117	**0.0357***

*$p < 0.05$. Bold p values.

HITS, Head Impact Telemetry System; DKI, diffusional kurtosis imaging; SD, standard deviation; BMI, body mass index; MK, mean kurtosis; RWEcp, Risk Weighted Cumulative Exposure combined probability; K axial, axial kurtosis; K radial, radial kurtosis.

the whole–brain (Table 1B; $p = 0.3507$). Covariate adjustment for age, BMI, and time between scans increased the strength of this relationship to explain 66% of variance ($p < 0.0001$). RWE_{CP} also demonstrated a significant relationship with AWF ($R^2 = 0.20$; $p = 0.0268$). The strength of this relationship increased after covariate adjustment for time between scans, age, and BMI ($R^2 = 0.51$; $p = 0.0013$). Other DKI-derived and WMM metrics (MK, K axial, K radial, and D_e axial, D_e radial, D_a) also achieved significance after covariate adjustment. The relationship between RWE_{CP} and its subcomponents with respect to tortuosity did not achieve significance. The linear component of RWE similarly achieved significance for many of these metrics, except for D_e axial (Table 1A; $p = 0.0675$). Relationships between RWE_{Linear} and whole–brain DKI-derived metrics (MK, K axial, and K radial) were all significant (Table 1B). For the rotational component of RWE, only whole–brain and gray matter DKI-derived metrics achieved significance (Tables 1B, 1D).

Tables 1A-D were computed based on two tails of the distribution, examining both increases and decreases (± 2 SD) in DKI-derived and WMM metrics. The metrics in Table 1A were calculated for areas where FA >0.4, whereas Table 1B includes all voxels within the brain. Table 1C is for WM voxels only and Table 1D is for gray matter voxels only. We performed additional analyses of the DKI-derived and WMM metrics examining only increases (+ 2 SD) shown in Tables 2A-D, and only decreases (- 2SD) shown in Tables 3A-D.

When only increases in MK (whole–brain) were considered (Table 2B), the relationships were similar to when both ends of the distribution were considered. The relationship between MK and RWE_{CP} explained 9.4% of the variance ($p = 0.1446$). After covariate adjustment, this relationship increased to explain 46.3% of the variance ($p = 0.0028$). The relationship between AWF and RWE_{CP} explained 21.3% of the variance ($p = 0.0232$), which increased after covariate adjustment to 39.4% of the variance ($p = 0.0081$).

When examining only decreases (Tables 3A-D), the relationship between MK and RWE_{CP} did not achieve significance. However, D_e radial was significant following covariate adjustment, as well as K radial in the WM. Similarly, for RWE_{linear}, only D_e axial and K axial in the white matter achieved significance following covariate adjustment. Interestingly, multiple metrics achieved significance for the rotational component ($RWE_{rotational}$), including AWF, D_e radial, MK, and K radial.

Total impacts

DKI-derived metrics, (MK, K axial, and K radial), compared with total impacts achieved significance only after covariate adjustment. For the WMM, D_e radial versus Total Impacts achieved significance when examining the decreases in white matter areas with FA >0.4. Other WMM metrics (AWF, tortuosity, D_e axial, and D_a) did not achieve a significant relationship, compared with total impacts.

Summed acceleration

DKI-derived metrics, (MK, K axial, and K radial), compared with summed linear acceleration, as well as summed rotational acceleration, achieved significance in gray matter and whole–brain only after covariate adjustment. Similar to total impacts, D_e radial versus summed linear acceleration and D_e radial versus summed rotational acceleration achieved significance when examining the decreases in white matter areas with FA >0.4. Other WMM metrics (AWF, tortuosity, D_e axial, and D_a) did not achieve a significant relationship, compared with summed linear acceleration or summed rotational acceleration.

Table 3A. Associations Between HITS Metrics and Changes in WMM Metrics in White Matter Areas With FA >0.4 (<–2SD)

	Without covariate adjustment		*Covariate adjustment for age, BMI, and time between scans*		
	R^2	*p value*	*Adjusted* R^2	*Covariate-adjusted* R^2	*p value*
AWF vs. RWE_{CP}	0.0488	0.2994	0.0343	0.1321	0.3415
Tortuosity vs. RWE_{CP}	0.1462	0.0652	0.1504	0.2696	0.1327
D_e axial vs. RWE_{CP}	0.0854	0.1659	0.1082	0.1638	0.1921
D_e radial vs. RWE_{CP}	0.1051	0.1222	0.4687	0.3756	**0.0025***
D_a vs. RWE_{CP}	0.1093	0.1146	0.1823	0.2421	0.0983
AWF vs. RWE_{Linear}	0.0847	0.1676	0.0903	0.1825	0.2227
Tort vs. RWE_{Linear}	0.0631	0.2364	0.0010	0.1487	0.4046
D_e axial vs. RWE_{Linear}	0.0475	0.3062	0.0786	0.1360	0.2447
D_e radial vs. RWE_{Linear}	0.0260	0.4517	0.4298	0.3299	**0.0047***
D_a vs. RWE_{Linear}	0.1053	0.1219	0.1745	0.2349	0.1059
AWF vs. $RWE_{Rotational}$	0.3069	**0.0050***	0.3562	0.4215	**0.0135***
Tortuosity vs. $RWE_{Rotational}$	0.1205	0.0965	0.0358	0.1710	0.3378
D_e axial vs. $RWE_{Rotational}$	0.0030	0.7997	0.0209	0.0819	0.3752
D_e radial vs. $RWE_{Rotational}$	0.0005	0.9213	0.3036	0.1816	**0.0264***
D_a vs. $RWE_{Rotational}$	0.0469	0.3094	0.0402	0.1105	0.3271
AWF vs. Total Impacts	0.0973	0.1379	0.0141	0.1140	0.3932
Tortuosity vs. Total Impacts	0.0166	0.5485	–0.1297	0.0287	0.8478
D_e axial vs. Total Impacts	0.0106	0.6314	–0.0018	0.0607	0.4369
D_e radial vs. Total Impacts	0.0014	0.8621	0.2599	0.1302	**0.0438***
D_a vs. Total Impacts	0.0708	0.2087	0.0362	0.1067	0.3368
AWF vs. summed linear acceleration	0.1128	0.1086	0.0628	0.1699	0.2766
Tortuosity vs. summed linear acceleration	0.0242	0.4684	–0.1063	0.0813	0.7730
D_e axial vs. summed linear acceleration	0.0107	0.6309	0.0057	0.1083	0.4160
D_e radial vs. summed linear acceleration	0.0001	0.9712	0.2986	0.3412	**0.0280***
D_a vs. summed linear acceleration	0.0414	0.1720	0.0817	0.1743	0.2387
AWF vs. summed rotational acceleration	0.0885	0.1580	0.0214	0.1262	0.3740
Tortuosity vs. summed rotational acceleration	0.0196	0.5138	–0.1175	0.0514	0.8095
D_e axial vs. summed rotational acceleration	0.0073	0.6912	–0.0064	0.0910	0.4502
D_e radial vs. summed rotational acceleration	0.0001	0.9928	0.2934	0.3265	**0.0298***
D_a vs. summed rotational acceleration	0.0738	0.1990	0.0662	0.1587	0.2694

*$p < 0.05$. Bold p values.

HITS, Head Impact Telemetry System; WMM, white matter modeling; FA, fractional anisotropy; SD, standard deviation; BMI, body mass index; AWF, axonal water fraction; RWEcp, Risk Weighted Cumulative Exposure combined probability; D_e axial and radial, extra-axonal diffusivity; D_a, intra-axonal diffusivity.

Cognitive testing

Spearman's rank correlation revealed no statistically significant associations between ImPACT composite score decrease (post-minus pre-season) and the number of abnormal voxels.

Discussion

In this study, we compared the pre- and post-season imaging data and cognitive data of players with head impact exposure experienced during one season of high school football, represented by RWE. A method was used allowing the number of abnormal DKI-derived metric voxels to be measured independent of spatial relationships. The number of abnormal voxels (> 2 SD) in all DKI-derived and most WMM metrics had a statistically significant association with RWE_{CP}. This study uses the same subjects and biomechanical data as a previous report investigating relationships between DTI-derived metrics and head impacts, allowing for direct comparison with the DTI data.[11] These studies are among the first to report quantitative relationships between head impact metrics and DTI-derived or DKI-derived scalars in non-concussed subjects.

The RWE metric captures the wide variances in exposure within the subjects. RWE_{CP} takes into account both the frequency and severity of the peak linear and rotational acceleration experienced from each impact to the head. RWE_{Linear} and $RWE_{Rotational}$ are computed from the peak linear and rotational accelerations separately. Each are computed from the respective risk function (combined probability, linear, or rotational). A positive relationship between an increasing RWE metric and an increasing number of abnormal DKI-derived and WMM metric voxels suggests an association between increased cumulative head impact exposure and white matter integrity changes. Studies in animal models and humans have shown the risk of brain injury and associated functional impairment increases as the frequency and severity of head impacts increase.[35–37] There are few studies relating DKI-derived or WMM metrics to TBI, or mTBI. However, it has been shown that DKI-derived metrics change in the presence of mTBI, especially MK.[21] Here, we demonstrate changes in DKI-derived and WMM metrics that are significantly associated with an athlete's cumulative head impact exposure, represented as RWE_{CP}, in the absence of clinically diagnosed concussion.

RWE_{CP} was able to explain variance in all DKI-derived and most WMM metrics. RWE_{Linear} was able to explain the variance in fewer metrics than those explained by RWE_{CP}. DKI-derived scalars demonstrated limited significant relationships with $RWE_{Rotational}$,

Table 3B. Associations Between HITS Metrics and Changes in DKI-Derived Metrics in Whole–Brain (< −2 SD)

	Without covariate adjustment		*Covariate adjustment for age, BMI, and time between scans*		
	R^2	*p value*	*Adjusted* R^2	*Covariate-adjusted* R^2	*p value*
MK vs. RWE_{CP}	0.0004	0.9282	0.1101	0.0338	0.1891
K axial vs. RWE_{CP}	0.0008	0.8971	0.0808	0.0114	0.2404
K radial vs. RWE_{CP}	0.0127	0.5995	0.1919	0.0898	0.0895
MK vs. RWE_{Linear}	0.0014	0.8618	0.1327	0.0584	0.1555
K axial vs. RWE_{Linear}	0.0062	0.7156	0.0983	0.0302	0.2087
K radial vs. RWE_{Linear}	0.0001	0.9601	0.2006	0.0997	0.0820
MK vs. $RWE_{Rotational}$	0.0264	0.4480	0.3915	0.3393	**0.0083***
K axial vs. $RWE_{Rotational}$	0.0024	0.8216	0.2380	0.1806	0.0556
K radial vs. $RWE_{Rotational}$	0.0205	0.5043	0.4340	0.3625	**0.0044***
MK vs. total impacts	0.0085	0.6683	0.1209	0.0456	0.1723
K axial vs. total impacts	0.0187	0.5235	0.0930	0.0245	0.2181
K radial vs. total impacts	0.0068	0.7018	0.1711	0.0664	0.1094
MK vs. summed linear acceleration	0.0075	0.6874	0.1309	0.1383	0.1580
K axial vs. summed linear acceleration	0.0176	0.5371	0.0984	0.0828	0.2084
K radial vs. summed linear acceleration	0.0058	0.7243	0.1818	0.1823	0.0988
MK vs. summed rotational acceleration	0.0084	0.6695	0.1222	0.1166	0.1703
K axial vs. summed rotational acceleration	0.0188	0.5233	0.0926	0.0654	0.2186
K radial vs. summed rotational acceleration	0.0056	0.7277	0.1751	0.1648	0.1053

*$p < 0.05$. Bold p values.

HITS, Head Impact Telemetry System; DKI, diffusional kurtosis imaging; SD, standard deviation; BMI, body mass index; MK, mean kurtosis; RWEcp, Risk Weighted Cumulative Exposure combined probability; K axial, axial kurtosis; K radial, radial kurtosis.

total impacts, or summed acceleration. We previously found that DTI-derived metrics were better explained by RWE_{CP} and demonstrated no relationship with total number of impacts.[11] RWE is an equation that includes not only the number of impacts or total acceleration, but the summed risk associated with the rotational and linear acceleration of each impact. The number of impacts or acceleration alone provide partial information, as the frequency and severity of impacts may have difference effects. RWE considers the non-linear relationship between impact magnitude and concussion risk and may be a more robust metric of characterizing the cumulative exposure of an athlete. Our findings with DKI metrics, again, suggest that knowledge of the cumulative exposure of an athlete,

Table 3C. Associations Between HITS Metrics and Changes in DKI-Derived Metrics in White Matter (< −2 SD)

	Without covariate adjustment		*Covariate adjustment for age, BMI, and time between scans*		
	R^2	*p value*	*Adjusted* R^2	*Covariate-adjusted* R^2	*p value*
MK vs. RWE_{CP}	0.0115	0.6179	0.0537	0.0909	0.2964
K axial vs. RWE_{CP}	0.0456	0.3163	0.2406	0.2192	0.0541
K radial vs. RWE_{CP}	0.1474	0.0640	0.4024	0.4194	**0.0071***
MK vs. RWE_{Linear}	0.0283	0.4317	0.1227	0.1572	0.1697
K axial vs. RWE_{Linear}	0.0307	0.4129	0.2750	0.2545	**0.0369***
K radial vs. RWE_{Linear}	0.0443	0.3233	0.2057	0.2283	0.0779
MK vs. $RWE_{Rotational}$	0.2378	**0.0156***	0.4957	0.5155	**0.0016***
K axial vs. $RWE_{Rotational}$	0.0352	0.3799	0.2230	0.2011	0.0652
K radial vs. $RWE_{Rotational}$	0.0612	0.2438	0.0713	0.0977	0.2590
MK vs. total impacts	0.0581	0.2564	0.1115	0.1464	0.1868
K axial vs. total impacts	0.0104	0.6354	0.1443	0.1201	0.1402
K radial vs. total impacts	0.0128	0.5984	0.0253	0.0530	0.3640
MK vs. summed linear acceleration	0.0578	0.2578	0.1418	0.2425	0.1435
K axial vs. summed linear acceleration	0.0144	0.5770	0.1873	0.2767	0.0936
K radial vs. summed linear acceleration	0.0170	0.5441	0.0554	0.1288	0.2926
MK vs. summed rotational acceleration	0.0466	0.3109	0.1113	0.2044	0.1872
K axial vs. summed rotational acceleration	0.0097	0.6464	0.1577	0.2323	0.1240
K radial vs. summed rotational acceleration	0.0197	0.5129	0.0572	0.1279	0.2886

*$p < 0.05$. Bold p values.

HITS, Head Impact Telemetry System; DKI, diffusional kurtosis imaging; SD, standard deviation; BMI, body mass index; MK, mean kurtosis; RWEcp, Risk Weighted Cumulative Exposure combined probability; K axial, axial kurtosis; K radial, radial kurtosis.

TABLE 3D. ASSOCIATIONS BETWEEN HITS METRICS AND CHANGES IN DKI-DERIVED METRICS IN GRAY MATTER (< −2 SD)

	Without covariate adjustment		*Covariate adjustment for age, BMI, and time between scans*		
	R^2	*p value*	*Adjusted* R^2	*Covariate-adjusted* R^2	*p value*
MK vs. RWE_{CP}	0.0001	0.9570	0.1327	0.0282	0.1555
K axial vs. RWE_{CP}	0.0020	0.8363	0.0654	0.0052	0.2712
K radial vs. RWE_{CP}	0.0094	0.6521	0.2139	0.0782	0.0717
MK vs. RWE_{Linear}	0.0047	0.7514	0.1466	0.0438	0.1373
K axial vs. RWE_{Linear}	0.0094	0.6518	0.0775	0.0181	0.2468
K radial vs. RWE_{Linear}	0.0005	0.9149	0.2153	0.0798	0.0707
MK vs. $RWE_{Rotational}$	0.0106	0.6321	0.3648	0.2883	**0.0121***
K axial vs. $RWE_{Rotational}$	0.0011	0.8801	0.2135	0.1628	0.0720
K radial vs. $RWE_{Rotational}$	0.0079	0.6787	0.4205	0.3205	**0.0054***
MK vs. total impacts	0.0220	0.4890	0.1326	0.0281	0.1557
K axial vs. total impacts	0.0250	0.4604	0.0746	0.0151	0.2524
K radial vs. total impacts	0.0185	0.5268	0.1860	0.0455	0.0948
MK vs. summed linear acceleration	0.0199	0.5107	0.1399	0.0978	0.1459
K axial vs. summed linear acceleration	0.0236	0.4735	0.0784	0.0525	0.2449
K radial vs. summed linear acceleration	0.0167	0.5468	0.1937	0.1383	0.0879
MK vs. summed rotational acceleration	0.0203	0.5068	0.1347	0.0815	0.1528
K axial vs. summed rotational acceleration	0.0247	0.4633	0.0744	0.0387	0.2529
K radial vs. summed rotational acceleration	0.0157	0.5590	0.1898	0.1256	0.0913

*$p < 0.05$. Bold p values.

HITS, Head Impact Telemetry System; DKI, diffusional kurtosis imaging; SD, standard deviation; BMI, body mass index; MK, mean kurtosis; RWEcp, Risk Weighted Cumulative Exposure combined probability; K axial, axial kurtosis; K radial, radial kurtosis.

represented by both the frequency and severity (linear and rotational acceleration) of each impact, is needed for accurate characterization of the effects of sub-concussive head impacts.

Changes in WMM metrics and DKI-derived metrics with regard to RWE may provide more information on the response of white matter to mTBI and subconcussive impacts. Water diffuses through biological tissues in a non-Gaussian manner due to cellular microstructure. This is also seen in the brain, especially due to myelinated axons. A higher mean kurtosis indicates more microstructural complexity. The axial and radial kurtosis provide the direction of any potential abnormalities. Tortuosity represents the ratio of diffusion along the direction of the fibers to diffusion perpendicular to the fibers in the EAS. Thus, tortuosity is a measure of the packing arrangement of the axons, not simply the packing density.[19] AWF represents the fraction of water signal in the axons relative to the total water signal. AWF values are comparable to axonal volume density measures in animal models.[34] D_e radial is expected to be sensitive to axonal volume, as well as myelin integrity. The D_e axial and D_a metrics should be sensitive to structural changes along, or parallel, the axon (e.g. axonal beading).[38]

In our study, we observed a significant relationship between cumulative exposure metrics and many of the DKI-derived and WMM metrics. These results indicate a variety of changes and injury types that may be occurring within the white matter, including axonal swelling, axonal beading, ischemia, and astrogliosis. Increases in AWF, indicating a greater amount of water in the axons relative to the total water signal post-season than pre-season, are indicative of axonal swelling. MK, K axial, and K radial all increased significantly for whole–brain, white matter, and gray matter. Similar changes have been seen previously in ischemic regions of stroke patients.[38,39] The significant increase in MK also has been demonstrated in axonal injury and astrogliosis.[25] Astrogliosis is the increase of reactive astrocytes due to the destruction of nearby neurons. This abnormal increase in astrocytes increases the microcellular complexity and has been shown to significantly elevate the measured MK in animal models.[25] The increase in astrocytes is a lingering effect seen in animal models after induced TBI.[40] Axonal injury and the associated release of cytokines by activated microglia can induce astrogliosis. Microglial inhibition is now the target of several potential and promising TBI therapies.[41–43]

Both significant increases and decreases were seen in the various WMM metrics. The trending decrease in D_a, in conjunction with the increase in AWF, follows a model of ischemia and is consistent with axonal beading.[38] The increases in D_a with decreases in D_e radial suggest areas of cytotoxic edema, causing water to shift from extra- to intra-axonal regions. In contrast, the increases in D_e axial and radial may be due to areas of extra-axonal inflammation or vasogenic edema. Interestingly, none of the results were suggestive of demyelination. In summary, our findings indicate that the axons are experiencing a variety of changes in their microstructural complexity. This may be indicative of multiple mechanisms, including swelling, beading, ischemia, and astrogliosis. However, the pathological implications of these metrics still are not well understood.

In all of these relationships, it is important to consider the strong effect of the covariates. DKI-derived metrics have proven to be a strong predictor of brain maturation, where DTI-derived metrics showed little dependency on age.[44,45] The DKI-derived metrics could be especially sensitive to the brain changes due to age and time between scans, making them important factors to regress out. However, the effect of BMI on DKI-derived metrics has not been well studied. There is evidence suggesting an effect of BMI on DTI-derived metrics.[46] A study of well characterized healthy children and animal models is necessary to further investigate these relationships.

In comparison to a previous study of DTI-derived metrics (obtained at the same imaging sessions in this exact same cohort), the DKI-derived scalar relationships with RWE explained more variance—especially D_a, MK, K axial, and K radial—in whole–brain

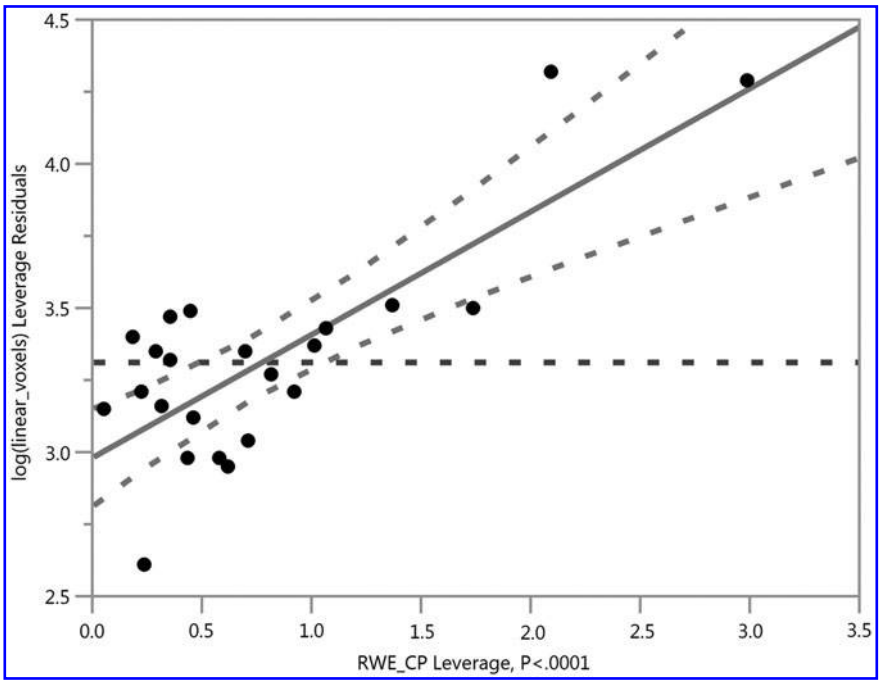

FIG. 1. Risk Weighted Cumulative Exposure combined probability (RWE_{CP}) vs. abnormal linear anisotropy (C_L) voxels in the white matter, adjusted for age, body mass index, and time between scans ($R^2 = 0.5626$; $p < 0.0001$).

and gray matter, suggesting that DKI may provide more sensitive and specific metrics for subconcussive head impacts. Our previous work with DTI in this group demonstrated the strongest relationship between linear anisotropy (C_L) and RWE_{CP} ($R^2 = 0.5626$; $p < 0.0001$), as shown in Figure 1. In the current study, the strongest relationships were between MK and RWE_{CP} ($R^2 = 0.6598$; $p < 0.0001$), as well as D_a and RWE_{CP} ($R^2 = 0.6412$; $p < 0.0001$), as shown in Figures 2 and 3. The relationship with C_L in our previous study suggested axotomy, or axonal tearing. The changes in D_a demonstrated here, however, are more suggestive of axonal beading and cytotoxic edema. The previous study demonstrated increases in spherical and planar diffusivities suggestive of

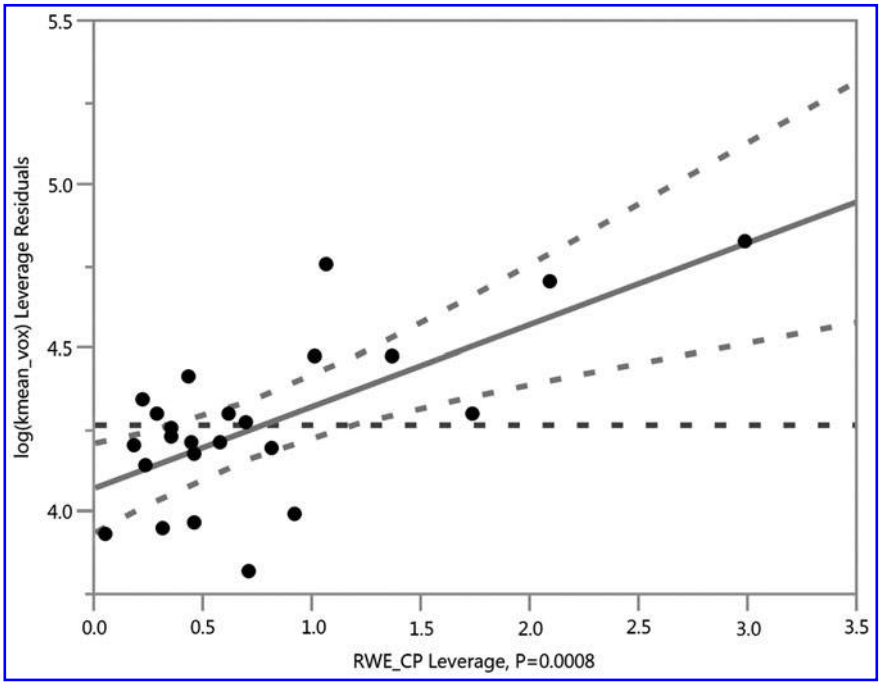

FIG. 2. Risk Weighted Cumulative Exposure combined probability (RWE_{CP}) vs. abnormal kurtosis (K) mean voxels in the whole–brain, adjusted for age, body mass index, and time between scans ($R^2 = 0.6598$; $p < 0.0001$).

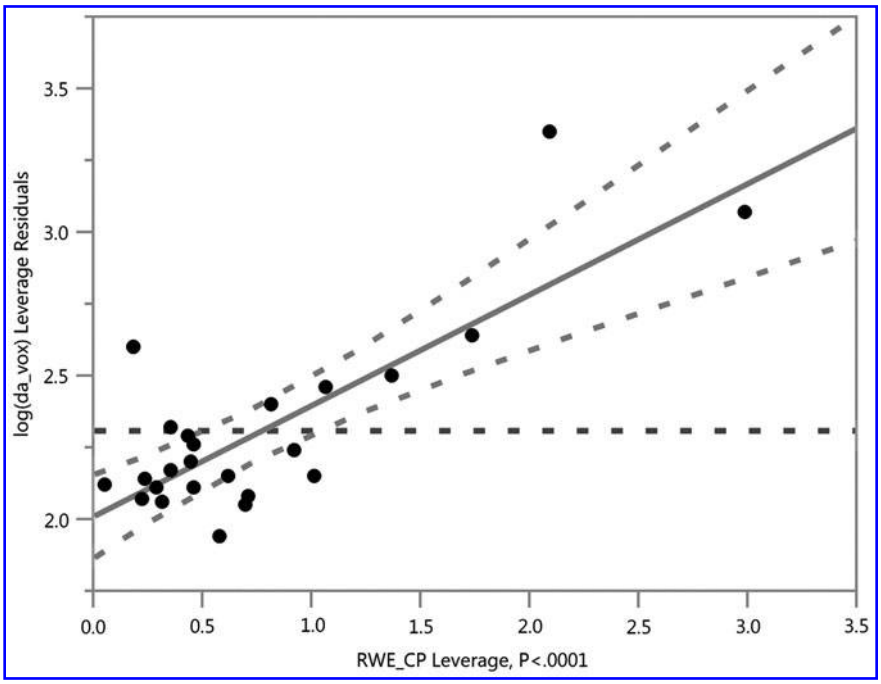

FIG. 3. Risk Weighted Cumulative Exposure combined probability (RWE_{CP}) vs. abnormal intra-axonal diffusivity (D_a) voxels in white matter areas with fractional anisotropy (FA) >0.4, adjusted for age, body mass index, and time between scans ($R^2 = 0.6412$; $p < 0.0001$).

demyelination. In contrast, we did not demonstrate evidence of demyelination in the DKI-derived metrics. This is not necessarily conflicting, as the DKI-derived metrics are more specific and can provide less ambiguous information. In addition, the relationship with MK and RWE_{CP} was suggestive of astrogliosis.

We found no statistically significant relationships between magnitude of delta ImPACT composite scores (post- minus pre-season) and number of abnormal voxels for any imaging metrics. We did demonstrate a significant relationship between Verbal Memory composite score and DTI metrics in our previous study.[11] It is known that DKI-derived metrics relate to cognitive metrics in Alzheimer's disease and mild cognitive impairment.[47] To identify this relationship in our cohort, a larger sample may be needed. In addition, the ImPACT test has proven sensitive to concussion, but its sensitivity to sub-concussive cognitive changes is unknown and the statistical power to detect associations may have been low.[48] The DKI metrics also may be demonstrating changes taking place in the brain before they become clinically apparent. This phenomena of the discrepancy between the amount of brain damage and the observed clinical manifestations is often described as cognitive reserve.[49]

Several caveats must be considered. Our sample size is relatively small; however, it is one of the largest studies to date of non-concussed high school football players to include biomechanics, imaging, and cognitive data. Our subjects were monitored during all practices and games by trained staff in concussion identification and management, including a certified athletic trainer. However, it is possible a concussion was not reported or went undetected, as previous studies show a 50% underreporting rate for concussion in high school football.[50] Although a control group of non-contact sport athletes was not used, this is somewhat mitigated by the use of delta metrics with the subjects baseline scans serving as an internal control. Our study was not designed to examine the potential reversibility or the time course of these changes. The WMM parameters are based on specific tissue modeling assumptions,[51] and so their interpretation should be regarded as preliminary.

Conclusion

We demonstrate a significant relationship between changes in DKI-derived metrics and cumulative head impact exposure using the RWE metric in the absence of clinical concussion. In this study, we show that a single season of high school football produced DKI-derived and WMM metric changes that have previously been seen in animal models of TBI. Although the pathophysiologic implications of these metrics will still require further research, this study adds to a growing body of literature demonstrating that a single season of contact sports can result in brain changes regardless of clinical findings or concussion diagnosis.

Acknowledgments

The authors would like to thank the Reagan High School, especially Ashley Lake, ATC, Corbin Ratcliffe, Lauren Smith, and the football program. Thank you to Ben Wagner and all those who contributed to the study development. Special thanks to the Childress Institute for Pediatric Trauma at Wake Forest Baptist Medical Center for providing support for this study. This material is based upon work supported by the National Science Foundation Graduate Research Fellowship under Grant No. DGE-0907738. Any opinion, findings, and conclusions or recommendations expressed in this material are those of the authors(s) and do not necessarily reflect the views of the National Science Foundation. Support for this research also was provided by National Institutes of Health grant NS082453 (JAM,JDS), NS088125 (JAM), and R01NS091602 (CTW, JAM, JDS).

References

1. Marar, M., McIlvain, N.M., Fields, S.K., and Comstock, R.D. (2012). Epidemiology of concussions among United States high school athletes in 20 sports. Am. J. Sports Med. 40, 747–755.
2. OTL: Pop Warner participation drops. Available at: http://espn.go.com/espn/otl/story/_/page/popwarner/pop-warner-youth-football-participation-drops-nfl-concussion-crisis-seen-causal-factor. Accessed April 20, 2016.
3. Brolinson, P.G., Manoogian, S., McNeely, D., Goforth, M., Greenwald, R., and Duma, S. (2006). Analysis of linear head accelerations from collegiate football impacts. Curr. Sports Med. Rep. 5, 23–28.
4. Duma, S.M., Manoogian, S.J., Bussone, W.R., Brolinson, P.G., Goforth, M.W., Donnenwerth, J.J., Greenwald, R.M., Chu, J.J., and Crisco, J.J. (2005). Analysis of real-time head accelerations in collegiate football players. Clin. J. Sport Med. 15, 3–8.
5. Schnebel, B., Gwin, J.T., Anderson, S., and Gatlin, R. (2007). In vivo study of head impacts in football: a comparison of National Collegiate Athletic Association Division I versus high school impacts. Neurosurgery 60, 490–495.
6. Guskiewicz, K.M., Mihalik, J.P., Shankar, V., Marshall, S.W., Crowell, D.H., Oliaro, S.M., Ciocca, M.F., and Hooker, D.N. (2007). Measurement of head impacts in collegiate football players: relationship between head impact biomechanics and acute clinical outcome after concussion. Neurosurgery 61, 1244–1252.
7. Urban, J.E., Davenport, E.M., Golman, A.J., Maldjian, J.A., Whitlow, C.T., Powers, A.K., and Stitzel, J.D. (2013). Head impact exposure in youth football: high school ages 14 to 18 years and cumulative impact analysis. Ann. Biomed. Eng. 41, 2474–2487.
8. Cobb, B.R., Urban, J.E., Davenport, E.M., Rowson, S., Duma, S.M., Maldjian, J.A., Whitlow, C.T., Powers, A.K., and Stitzel, J.D. (2013). Head impact exposure in youth football: elementary school ages 9–12 years and the effect of practice structure. Ann. Biomed. Eng. 41, 2463–2473.
9. Wong, R.H., Wong, A.K., and Bailes, J.E. (2014). Frequency, magnitude, and distribution of head impacts in Pop Warner football: the cumulative burden. Clin. Neurol. Neurosurg. 118, 1–4.
10. Mills, K.L. and Tamnes, C.K. (2014). Methods and considerations for longitudinal structural brain imaging analysis across development. Dev. Cogn. Neurosci. 9, 172–190.
11. Davenport, E.M., Whitlow, C.T., Urban, J.E., Espeland, M.A., Jung, Y., Rosenbaum, D.A., Gioia, G.A., Powers, A.K., Stitzel, J.D., and Maldjian, J.A. (2014). Abnormal white matter integrity related to head impact exposure in a season of high school varsity football. J. Neurotrauma 31, 1617–1624.
12. Bazarian, J.J., Zhu, T., Zhong, J., Janigro, D., Rozen, E., Roberts, A., Javien, H., Merchant-Borna, K., Abar, B., and Blackman, E.G. (2014). Persistent, long-term cerebral white matter changes after sports-related repetitive head impacts. PLoS One 9, e94734.
13. DeCarlo, L.T. (1997). On the meaning and use of kurtosis. Psychol. Methods 2, 292–307.
14. Jensen, J.H., and Helpern, J.A. (2010). MRI quantification of non-Gaussian water diffusion by kurtosis analysis. NMR Biomed. 23, 698–710.
15. Jensen, J.H., Helpern, J.A., Ramani, A., Lu, H., and Kaczynski, K. (2005). Diffusional kurtosis imaging: The quantification of non-gaussian water diffusion by means of magnetic resonance imaging. Magn. Reson. Med. 53, 1432–1440.
16. Jensen, J.H. and Helpern, J.A. (2010). MRI quantification of non-Gaussian water diffusion by kurtosis analysis. NMR Biomed. 23, 698–710.
17. Lazar, M. (2010). Mapping brain anatomical connectivity using white matter tractography. NMR Biomed. 23, 821–835.
18. Hui, E.S., Russell Glenn, G., Helpern, J.A., and Jensen, J.H. (2015). Kurtosis analysis of neural diffusion organization. NeuroImage 106, 391–403.
19. Jelescu, I.O., Veraart, J., Adisetiyo, V., Milla, S.S., Novikov, D.S., and Fieremans, E. (2015). One diffusion acquisition and different white matter models: how does microstructure change in human early development based on WMTI and NODDI? NeuroImage 107, 242–256.
20. Lazar, M., Miles, L.M., Babb, J.S., and Donaldson, J.B. (2014). Axonal deficits in young adults with High Functioning Autism and their impact on processing speed. NeuroImage: Clin. 4, 417–425.
21. Stokum, J.A., Sours, C., Zhuo, J., Kane, R., Shanmuganathan, K., and Gullapalli, R.P. (2015). A longitudinal evaluation of diffusion kurtosis imaging in patients with mild traumatic brain injury. Brain Inj. 29, 47–57.
22. Adisetiyo, V., Tabesh, A., Di Martino, A., Falangola, M.F., Castellanos, F.X., Jensen, J.H., and Helpern, J.A. (2014). Attention-deficit/hyperactivity disorder without comorbidity is associated with distinct atypical patterns of cerebral microstructural development. Hum. Brain Mapp. 35, 2148–2162.
23. Fieremans, E., Benitez, A., Jensen, J.H., Falangola, M.F., Tabesh, A., Deardorff, R.L., Spampinato, M.V.S., Babb, J.S., Novikov, D.S., Ferris, S.H. and Helpern, J.A. (2013). Novel white matter tract integrity metrics sensitive to Alzheimer disease progression. A.J.N.R. Am. J. Neuroradiol. 34, 2105–2112.
24. Grossman, E.J., Jensen, J.H., Babb, J.S., Chen, Q., Tabesh, A., Fieremans, E., Xia, D., Inglese, M., and Grossman, R.I. (2013). Cognitive impairment in mild traumatic brain injury: a longitudinal diffusional kurtosis and perfusion imaging study. A.J.N.R. Am. J. Neuroradiol. 34, 951–957, S951–953.
25. Zhuo, J., Xu, S., Proctor, J.L., Mullins, R.J., Simon, J.Z., Fiskum, G., and Gullapalli, R.P. (2012). Diffusion kurtosis as an in vivo imaging marker for reactive astrogliosis in traumatic brain injury. NeuroImage 59, 467–477.
26. Broglio, S.P., Sosnoff, J.J., Shin, S., He, X., Alcaraz, C., and Zimmerman, J. (2009). Head impacts during high school football: a biomechanical assessment. J Athl Train 44, 342–349.
27. Daniel, R.W., Rowson, S., and Duma, S.M. (2012). Head impact exposure in youth football. Ann. Biomed. Eng. 40, 976–981.
28. Rowson, S. and Duma, S.M. (2013). Brain injury prediction: assessing the combined probability of concussion using linear and rotational head acceleration. Ann. Biomed. Eng. 41, 873–882.
29. Rowson, S., Duma, S.M., Beckwith, J.G., Chu, J.J., Greenwald, R.M., Crisco, J.J., Brolinson, P.G., Duhaime, A.C., McAllister, T.W., and Maerlender, A.C. (2012). Rotational head kinematics in football impacts: an injury risk function for concussion. Ann. Biomed. Eng. 40, 1–13.
30. M.R. Lovell, M.W.C., K. Podell, J. Powell, J. Maroon (2000). *ImPACT: Immediate Post-Concussion Assessment and Cognitive Testing*. NeuroHealth Systems, LLC: Pittsburgh.
31. Maroon, J.C., Lovell, M.R., Norwig, J., Podell, K., Powell, J.W., and Hartl, R. (2000). Cerebral concussion in athletes: evaluation and neuropsychological testing. Neurosurgery 47, 659–669.
32. Smith, S.M., Jenkinson, M., Woolrich, M.W., Beckmann, C.F., Behrens, T.E., Johansen-Berg, H., Bannister, P.R., De Luca, M., Drobnjak, I., Flitney, D.E., Niazy, R.K., Saunders, J., Vickers, J., Zhang, Y., De Stefano, N., Brady, J.M., and Matthews, P.M. (2004). Advances in functional and structural MR image analysis and implementation as FSL. NeuroImage 23 Suppl 1, S208–S219.
33. Tabesh, A., Jensen, J.H., Ardekani, B.A., and Helpern, J.A. (2011). Estimation of tensors and tensor-derived measures in diffusional kurtosis imaging. Magn. Reson. Med. 65, 823–836.
34. Fieremans, E., Jensen, J.H., and Helpern, J.A. (2011). White matter characterization with diffusional kurtosis imaging. NeuroImage 58, 177–188.
35. Ommaya, A.K. and Hirsch, A.E. (1971). Tolerances for cerebral concussion from head impact and whiplash in primates. J. Biomech. 4, 13–21.
36. Ono, K., Kikuchi, A., Nakamura, M., Kobayashi, H., and Nakamura, N. (1980). *Human Head Tolerance to Sagittal Impact Reliable Estimation Deduced from Experimental Head Injury Using Subhuman Primates and Human Cadaver Skulls.* SAE Technical Paper 801303.
37. Rowson, S. and Duma, S.M. (2013). Brain injury prediction: assessing the combined probability of concussion using linear and rotational head acceleration. Ann. Biomed. Eng. 41, 873–882.
38. Hui, E.S., Fieremans, E., Jensen, J.H., Tabesh, A., Feng, W., Bonilha, L., Spampinato, M.V., Adams, R., and Helpern, J.A. (2012). Stroke assessment with diffusional kurtosis imaging. Stroke 43, 2968–2973.
39. Jensen, J.H., Falangola, M.F., Hu, C., Tabesh, A., Rapalino, O., Lo, C., and Helpern, J.A. (2011). Preliminary observations of increased diffusional kurtosis in human brain following recent cerebral infarction. NMR Biomed. 24, 452–457.
40. Shitaka, Y., Tran, H.T., Bennett, R.E., Sanchez, L., Levy, M.A., Dikranian, K., and Brody, D.L. (2011). Repetitive closed-skull traumatic brain injury in mice causes persistent multifocal axonal injury and microglial reactivity. J. Neuropathol. Exp. Neurol. 70, 551–567.
41. Giovanni, S.D., Movsesyan, V., Ahmed, F., Cernak, I., Schinelli, S., Stoica, B., and Faden, A.I. (2005). Cell cycle inhibition provides

neuroprotection and reduces glial proliferation and scar formation after traumatic brain injury. Proc. Natl. Acad. Sci. U.S.A. 102, 8333–8338.
42. Erlich, S., Alexandrovich, A., Shohami, E., and Pinkas-Kramarski, R. (2007). Rapamycin is a neuroprotective treatment for traumatic brain injury. Neurobiol. Dis. 26, 86–93.
43. Zhang, D., Hu, X., Qian, L., O'Callaghan, J.P., and Hong, J.-S. (2010). Astrogliosis in CNS pathologies: is there a role for microglia? Mol. Neurobiol. 41, 232–241.
44. Das, S.K., Wang, J.L., Bing, L., Bhetuwal, A., and Yang, H.F. (2016). Regional values of diffusional kurtosis estimates in the healthy brain during normal aging. Clin. Neuroradiol. 2016 Jan 4; Epub ahead of print.
45. Cheung, M.M., Hui, E.S., Chan, K.C., Helpern, J.A., Qi, L., and Wu, E.X. (2009). Does diffusion kurtosis imaging lead to better neural tissue characterization? A rodent brain maturation study. Neuroimage 45, 386–392.
46. Kullmann, S., Callaghan, M.F., Heni, M., Weiskopf, N., Scheffler, K., Haring, H.U., Fritsche, A., Veit, R., and Preissl, H. (2016). Specific white matter tissue microstructure changes associated with obesity. Neuroimage 125, 36–44.
47. Benitez, A., Fieremans, E., Jensen, J.H., Falangola, M.F., Tabesh, A., Ferris, S.H., and Helpern, J.A. (2014). White matter tract integrity metrics reflect the vulnerability of late-myelinating tracts in Alzheimer's disease. NeuroImage Clin. 4, 64–71.
48. Schatz, P. and Sandel, N. (2013). Sensitivity and specificity of the online version of ImPACT in high school and collegiate athletes. Am. J. Sports Med. 41, 321–326.
49. Stern, Y. (2009). Cognitive reserve. Neuropsychologia 47, 2015–2028.
50. McCrea, M., Hammeke, T., Olsen, G., Leo, P., and Guskiewicz, K. (2004). Unreported concussion in high school football players: implications for prevention. Clin. J. Sports Med. 14, 13–17.
51. Dhital B, K.E., Reisert M, Kiselev VG (2015). Isotropic Diffusion Weighting Provides Insight on Diffusion Compartments in Human Brain White Matter In vivo. In: ISMRM 23rd Annual Meeting & Exhibition. Proc. Intl. Soc. Mag. Reson. Med.: Toronto, Ontario, Canada, pps. 2788.

Address correspondence to:
Christopher T. Whitlow, MD, PhD, MHA
Department of Radiology-Neuroradiology
Translational Science Institute
Advanced Neuroscience Imaging Research Core
Wake Forest University Health Sciences
Winston-Salem, NC 27157-1088

E-mail: cwhitlow@wakehealth.edu

This article has been cited by:

1. Jens H. Jensen, Emilie T. McKinnon, G. Russell Glenn, Joseph A. Helpern. 2017. Evaluating kurtosis-based diffusion MRI tissue models for white matter with fiber ball imaging. *NMR in Biomedicine* **30**:5, e3689. [CrossRef]
2. Yu Fengshan , 1, 2 Shukla Dinesh K. , 1, 5 Armstrong Regina C. , 1, 2, 3 Marion Christina M. , 1, 3 Radomski Kryslaine L. , 1, 2 Selwyn Reed G. , 1, 6, * and Dardzinski Bernard J. 1, 4, * 1Center for Neuroscience and Regenerative Medicine, Uniformed Services University of the Health Sciences, Bethesda, Maryland. 2Department of Anatomy, Physiology and Genetics, Uniformed Services University of the Health Sciences, Bethesda, Maryland. 3Program in Neuroscience, Uniformed Services University of the Health Sciences, Bethesda, Maryland. 4Department of Radiology and Radiological Sciences, Uniformed Services University of the Health Sciences, Bethesda, Maryland. 5Department of Psychiatry, University of Maryland School of Medicine, Baltimore, Maryland. 6Department of Radiology, University of New Mexico, Albuquerque, New Mexico. . 2017. Repetitive Model of Mild Traumatic Brain Injury Produces Cortical Abnormalities Detectable by Magnetic Resonance Diffusion Imaging, Histopathology, and Behavior. *Journal of Neurotrauma* **34**:7, 1364-1381. [Abstract] [Full Text HTML] [Full Text PDF] [Full Text PDF with Links] [Supplemental Material]
3. Svetlana A. Dambinova, Joseph C. Maroon, Alicia M. Sufrinko, John David Mullins, Eugenia V. Alexandrova, Alexander A. Potapov. 2016. Functional, Structural, and Neurotoxicity Biomarkers in Integrative Assessment of Concussions. *Frontiers in Neurology* **7**. . [CrossRef]